

Keitaro Ohno · Roberto Horowitz

## A pivot nonlinearity compensation by use of variable structure estimator for hard disk drives

Received: 30 June 2003 / Accepted: 21 April 2004 / Published online: 18 August 2005  
© Springer-Verlag 2005

**Abstract** This paper discusses robust seeking control of hard disk drives by the use of a variable structure multi-rate estimator (VSME). Compensation of pivot nonlinearity is one concern in the design of the seeking control systems. Pivot nonlinearity is subject to uncertainties, and is difficult to deal with by a linear controller. The VSME estimates a class of uncertain disturbances and nonlinearities and yields compensation current through the linear feedback gain, which reduces the residual vibration and error during settling. Several experiments were carried out on several drives including a 3.5 in. 7,200 rpm drive. These experiments confirmed that the off-track probability after settling, which is defined by the number of seek failures over all trials, is much reduced to less than 1% when the drive is operated under a special temperature condition that increases pivot nonlinearity while the corresponding performance of a conventional linear controller is 12%. The seek failure is defined as the case when the position cannot be maintained within  $\pm 2.5\%$  of a track pitch for a certain duration after track seeking mode.

### 1 Introduction

The positioning mechanism of hard disk drives (HDDs) consists of magnetic disks, magnetic heads, arms, and a voice coil motor (VCM), as shown in Fig. 1. On the magnetic disk, position data is embedded like the spokes

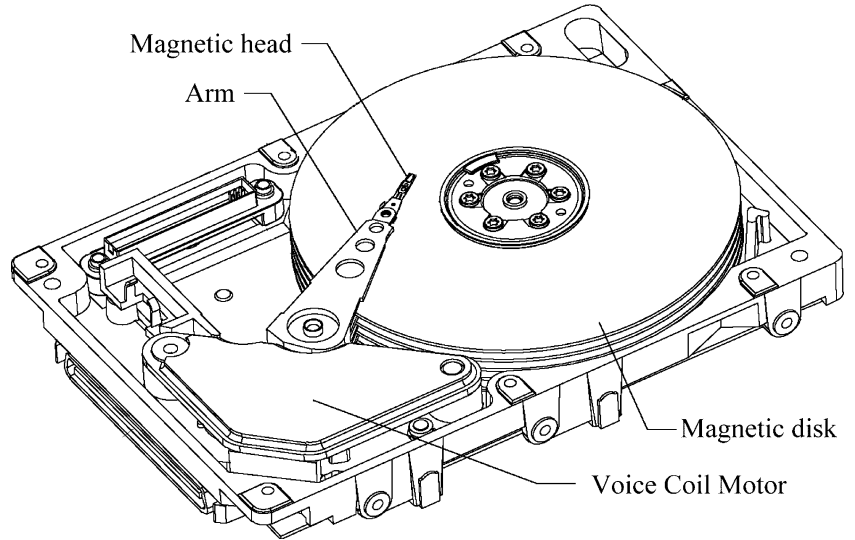
of a wheel, and the position error signal (PES) can be obtained from this position data when the head crosses the servo frame. Thus, the control system of a normal HDD must inevitably be a sampled-data control system; with a single input as the current of VCM and single output as the PES. Moreover, its sampling frequency is limited since increasing the number of embedded position data results in losing the available data capacity. Under such conditions, utilization of multi-rate feedback control for HDDs was proposed (Chiang 1990), and since then many authors have discussed this issue for track following control (Hara and Tomizuka 1998; Takiguchi et al. 2002; Ishikawa 2000; Semba 2001; Ohno et al. 2001) and it is successfully used in industry. However, as (Ishikawa and Tomizuka 1998) pointed out, the compensation of nonlinearity and uncertainty remains a key concern for further performance enhancement. One clear example is that the actuator has nonlinearity such as friction, flexible-printed-cable tension, which have shown to affect the servo performance of HDDs by creating a torque bias (Prater et al. 1996) and many authors have tried to overcome this problem. One way is to utilize the disturbance observer scheme (e.g. Nakagawa and Hamada 1996), by using the PES and input current. This scheme is simple and effective. However, its performance depends on the accuracy of the nonlinearity model since it is subject to uncertainty. Ishikawa and Tomizuka (1998) propose a way of compensation by the use of an accelerometer with a modified version of a regular disturbance observer. This overcomes the drawback of the previous method; however, an additional sensor is needed.

In this paper, a variable structure multi-rate estimator (VSME) is proposed for pivot nonlinearity compensation. The basic idea of the estimator is to combine the variable structure estimator (Walcott and Zak 1987) and integral observer (Beale and Shafai 1989; Shafai and carrol 1985), and to put them into a multi-rate state estimator framework (Hara and Tomizuka 1998). The observer in Walcott and Zak (1987) provides active robustness against parameter uncertainty, which also

K. Ohno (✉)  
Autonomous System Laboratory,  
Fujitsu Laboratories Limited, Atsugi 243-0197, Japan  
E-mail: keitaro.ohno@nifty.com

R. Horowitz  
Department of Mechanical Engineering,  
University of California, Berkeley, CA 94720-1740, USA  
E-mail: horowitz@me.berkeley.edu

**Fig. 1** Hard disk drives (HDDs)



reduces the spill-over problem caused by unmodeled dynamics because there is no unmodeled dynamics in the estimator loop, while the multi-rate estimator technique smoothes the inter-sample estimation. The integral action reduces the upper bound estimate of the uncertainty that is used to design the discontinuous action. Thus, a class of nonlinearity and uncertainty including pivot nonlinearity can be dealt with by this method.

## 2 Variable structure multi-rate estimator

The controlled plant we consider in this paper is described as follows.

$$\begin{aligned} \dot{x}(t) &= Ax(t) + Bu(t) + w_c(x, u, t), \\ y(t) &= Cx(t), \end{aligned} \quad (1)$$

where,  $x \in \mathbf{R}^n$ ,  $y \in \mathbf{R}^p$ ,  $u \in \mathbf{R}^m$ ,  $A \in \mathbf{R}^{n \times n}$ ,  $B \in \mathbf{R}^{n \times m}$ ,  $C \in \mathbf{R}^{p \times n}$ . We assume that the pair  $(A, B)$  is controllable, the pair  $(A, C)$  is observable, and  $B, C$  are both full rank. The function  $w_c : \mathbf{R}^n \times \mathbf{R}^m \times \mathbf{R}_+ \rightarrow \mathbf{R}^n$  represents any uncertainty. Furthermore, we ignore time delay for simplicity. Then, the equivalent multi-rate system can be written as follows.

$$\begin{aligned} x(k, i+1) &= \Phi_m x(k, i) + \Gamma_m u(k, i) + w(x, u, k) \\ y(k, i) &= Cx(k, 0) \end{aligned} \quad (2)$$

where,  $\Phi_m \in \mathbf{R}^{n \times n}$  and  $\Gamma_m \in \mathbf{R}^{n \times m}$  can be written as follows.

$$\Phi_m = e^{AT_m}, \quad \Gamma_m = \int_0^{T_m} e^{At} dt B \quad (3)$$

where  $T_m$  is a control update period, which is described as  $T_m = T_s / r$ ,  $T_s$  being the measurement sampling period, and  $r$  being multi-rate ratio. The pair  $(k, i)$  denotes the time  $t = kT_s + iT_m$ ,  $i = 0, 1, \dots, r - 1$ . The function  $w_c : \mathbf{R}^n \times \mathbf{R}^m \times \mathbf{N}_+ \rightarrow \mathbf{R}^n$  represents any uncertainty that comprises an average behavior and a fluctuating behavior, each of which is respectively within the range space of some full rank matrices,  $\Theta_B \in \mathbf{R}^{n \times q}$  and  $\Theta_D \in \mathbf{R}^{n \times d}$ . Thus  $w$  in Eq. 2 can be described as follows.

$$w(x, u, k) = \Theta_B h + \Theta_D \delta h(x, u, k), \quad (4)$$

where  $h \in \mathbf{R}^q$  and  $\delta h \in \mathbf{R}^d$  are respectively the average and fluctuating behaviors of the uncertainty, and we assume  $q \leq p$  and  $d \leq p$ . Also, the upper bound of  $\delta h$  is assumed to be known as follows:

$$\|\delta h(x, u, k)\| < h^+(x, u, k), \quad (5)$$

where  $h^+ : \mathbf{R}^n \times \mathbf{R}^m \times \mathbf{N}_+ \rightarrow \mathbf{R}_+$  is a known scalar function. In addition, the higher frequency component of the behavior of  $\delta h$  is assumed to be ignorable.

Throughout this paper,  $\rho(\cdot)$ ,  $\lambda$ ,  $\sigma$ , and  $|\cdot|$  respectively denote the spectral radius, the eigenvalue, the singular value, and Euclidian norm for vectors and spectral norm for matrices. For other notations, we will use standard mathematical expressions.

Figure 2 shows the overall proposed control system. The structure of the proposed estimator is as follows.

$$\begin{cases} \bar{x}(k, i+1) = \Phi_m \hat{x}(k, i) + \Gamma_m u(k, i) \\ \bar{z}(k+1, 0) = \hat{z}(k, 0) \end{cases} \quad (6)$$

$$\begin{cases} \hat{x}(k, i) = \bar{x}(k, i) + L_i \{y(k, 0) - C\bar{x}(k, 0)\} + \Theta_b \hat{z}(k, 0) + \Theta_d v(k, 0) \\ \hat{z}(k, 0) = \bar{z}(k, 0) + K \{y(k, 0) - C\bar{x}(k, 0)\} \end{cases} \quad (7)$$



$$\bar{e}_z(k+1) = \Psi_{\text{obs}} \bar{e}_z(k) + \begin{bmatrix} Yw \\ O \end{bmatrix} \quad (11)$$

where  $w$  in this case is assumed to be constant and given by  $w = \Theta_B h$ . The characteristics equation for nominal linear system can be derived as follows.

$$\det(zI - \Psi_{\text{obs}}) = 0. \quad (12)$$

On the other hand, regarding the dynamics for current estimation error, from Eq. 6 and the relation:  $\bar{e} = \hat{e} - \bar{x} + \hat{x}$ , we have the following relation.

$$\bar{e}(k, 0) = X^{-1} \hat{e}(k, 0) + X^{-1} \Theta_b \hat{z}(k-1, 0), \quad (13)$$

$$\Leftrightarrow \bar{e}_z(k) = \Omega \hat{e}_z(k), \quad (14)$$

where  $X$  is assumed invertible. Note that  $X$  can be designed to be invertible by the proper choice of the gain  $L_0$  and  $K$ . By substituting Eq. 14 into Eq. 11, we obtain the dynamics for current estimation error.

$$\hat{e}_z(k+1) = \Omega^{-1} \Psi_{\text{obs}} \Omega \hat{e}_z(k) + \Omega^{-1} \begin{bmatrix} Yw \\ O \end{bmatrix}. \quad (15)$$

From the above relation, we have the following characteristics equation for the nominal linear system

$$\det(zI - \Phi_{\text{obs}}) = \det\{\Omega^{-1}(zI - \Psi_{\text{obs}})\Omega\} = \det(zI - \Psi_{\text{obs}}) = 0 \quad (16)$$

Thus, both error dynamics have the same eigenvalues. Notice that, from Eq. 11, we can see that the error dynamics of  $\bar{e}$  in  $\bar{e}_z$  has an additional term given by  $N\bar{z}$  due to the I-action, which can handle the constant disturbance term  $Yw$  in Eq. 11 and  $h$  is cancelled out by the I-action estimator,  $\bar{z}$ , by letting  $\Theta_b = \Phi_m^{-1} \Theta_B$ . Note that  $\Phi_m$  is always nonsingular since  $T_m$  is nonzero in Eq. 3.

Now, we can design the estimation gain matrices ( $K$ ,  $L_i$ ) in Eq. 11 by invoking some conventional direct pole placement techniques.

$$\bar{e}_z(k+1) = \begin{bmatrix} \Phi_m^r & N \\ O & I \end{bmatrix} \bar{e}_z(k) - \begin{bmatrix} \sum_{j=1}^r \Phi_m^j (L_{r-j} + \Theta_b K) \\ -K \end{bmatrix} [CO] \bar{e}_z(k), \quad (17)$$

where it is assumed that there is no invariant zero at  $z=1$  for the triple  $(\Phi_m^r, N, C)$ , which corresponds to the system triple from the input signal  $h$  to the output  $y$ .

## 2.2 Variable structure part design of VSME

Let us first begin with establishing the stability of the overall nonlinear estimator. When the discontinuous action is considered, Eq. 11 becomes as follows.

$$\bar{e}_z(k+1) = \Psi_{\text{obs}} \bar{e}_z(k) + \begin{bmatrix} Y(w + \Phi_m \Theta_d v) \\ O \end{bmatrix}, \quad (18)$$

where we assume in this case that  $w$  is given by Eq. 4. Thus, from Eq. 18 we can understand that some freedom is added to the system to alleviate the detrimental effect of  $\delta h$ , by setting  $\Theta_d = \Phi_m^{-1} \Theta_D$ , where  $\Theta_D$  is defined in Eq. 4.

The stability of this estimator can be established as follows. First, consider the following coordinate transformation in order to evaluate the integral state  $\bar{z}$  at the origin.

$$\bar{e}_z \mapsto e_{zw} := [\bar{e}^T \quad (\bar{z} - h)^T]^T \quad (19)$$

By using this coordinate transformation, Eq. 18 can be rewritten as follows:

$$e_{zw}(k+1) = \Phi_{\text{obs}} e_{zw}(k) + \Theta_z \delta h(k) + \Theta_z v(k). \quad (20)$$

Define the Lyapunov function candidate as follows:

$$V_{\text{obs}}(k) = e_{zw}^T(k) P_z e_{zw}(k) = e_{zw}^T P_z e_{zw} \quad (21)$$

where  $P_z$  is positive definite. Evaluate Eq. 20 along its trajectory as follows:

$$\begin{aligned} V_{\text{obs}}(k+1) - V_{\text{obs}}(k) &= e_{zw}^T (\Psi_{\text{obs}}^T P_z \Psi_{\text{obs}} - P_z) e_{zw} \\ &\quad + \delta h^T \Theta_z^T P_z \Theta_z \delta h \\ &\quad + v^T \Theta_z^T P_z \Theta_z v + 2e_{zw}^T \Psi_{\text{obs}}^T P_z \Theta_z \delta h + 2e_{zw}^T \Psi_{\text{obs}}^T P_z \Theta_z v \\ &\quad + 2\delta h^T \Theta_z^T P_z \Theta_z v \\ &\leq -e_{zw}^T Q_z e_{zw} + \|\Theta_z^T P_z \Theta_z\| (\|\delta h\|^2 + \kappa^2) \\ &\quad + 2e_{zw}^T C_z^T D^T \delta h - 2e_{zw}^T C_z^T D^T \kappa \frac{DC_z e_{zw}}{\|DC_z e_{zw}\|} \\ &\quad - 2\delta h^T \Theta_z^T P_z \Theta_z \kappa \frac{DC_z e_{zw}}{\|DC_z e_{zw}\|} \\ &\leq -\lambda_{\min}(Q_z) \|e_{zw}\|^2 + \|\Theta_z^T P_z \Theta_z\| (\|\delta h\|^2 + \kappa^2) \\ &\quad + 2\|DC_z e_{zw}\| (h^+ - \kappa) - 2\delta h^T \Theta_z^T P_z \Theta_z \kappa \frac{DC_z e_{zw}}{\|DC_z e_{zw}\|} \\ &< -\lambda_{\min}(Q_z) \|e_{zw}\|^2 + \|\Theta_z^T P_z \Theta_z\| (\|\delta h\|^2 + \kappa^2) \\ &\quad - 2\delta h^T \Theta_z^T P_z \Theta_z \kappa \frac{DC_z e_{zw}}{\|DC_z e_{zw}\|} \\ &< -\lambda_{\min}(Q_z) \|e_{zw}\|^2 + \|\Theta_z^T P_z \Theta_z\| (h^+ + \kappa)^2. \end{aligned}$$

Since  $Q_z$  is positive definite, the above evaluation is upper convex with respect to  $e_{zw}$ . Thus there always exist an ultimately bounded sliding mode estimator, and the estimation error can be confined within the space given by

$$E = \left\{ e_{zw} \in \mathbf{R}^{n+g} : \|e_{zw}\| < 2\sqrt{\frac{\lambda_{\max}(\Theta_z^T P_z \Theta_z)}{\lambda_{\min}(Q_z)}} \kappa \right\}. \quad (22)$$

If the signum of switching function is different from that of the uncertainty, the discontinuous term is feedback so that states go to the same direction as the uncertainty and the discontinuous action does more harm than good. This can be easily understood by thinking of a fast varying uncertainty whose frequency is almost the same as Nyquist frequency. Thus, for

practical design purpose, some measures to avoid this situation should be taken. One way is to apply a band-limit filter to the discontinuous action of  $v$  in Eq. 8, and also introduce a saturation function or other kind of function so as to alleviate the chattering motion, as we will demonstrate in the following experiments. Furthermore, for single output applications, it is obvious from the Eq. 8 that we can set  $D=1$  without loss of generality since  $p=1$  implies  $d=1$  and it follows  $D \in \mathbf{R}$ . In this case, the sliding mode always takes place on the error space given by  $\{\bar{e}_z \in \mathbf{R}^{n+1} : C_z \bar{e}_z = 0\}$ .

### 2.3 Regulator design

From the theoretical point of view, in order to cancel out the uncertainty that exists in the closed-loop system, we have to also consider its cancellation in the regulator design in addition to the estimator design. However, from the practical design point of view, it is not desirable to introduce an additional discontinuous action into the control loop for HDDs since it directly deteriorates the positioning accuracy. Thus, a sliding mode-based regulator is designed within a linear control system design framework, which still achieves better robustness against uncertainty as compared with a standard HDD seek design.

First, the discrete-time switching function,  $S(k, i) \in \mathbf{R}^m$ , is defined with a reference input,  $x_r \in \mathbf{R}^n$ , as follows:

$$S(k, i) = G\{x(k, i) + x_r(k, i)\}, \quad (23)$$

where  $G \in \mathbf{R}^{m \times n}$  is a sliding hyperplane matrix. Then, we propose the following condition:

$$\begin{aligned} S(k+1) &= \alpha S(k) \\ \alpha &= \text{diag}(\alpha_1, \alpha_2, \dots, \alpha_m), \quad 0 \leq \alpha_1, \alpha_2, \dots, \alpha_m < 1, \end{aligned} \quad (24)$$

where  $\alpha \in \mathbf{R}^{m \times m}$  is a design constant. This condition implies that a sliding hyperplane itself does not have dynamics, but the switching function can be thought of as having a first order dynamics without the need to introduce an additional state. Therefore,  $\alpha$  can be designed as follows:

$$\alpha_j = \exp(-2\pi f_j T_m), \quad (25)$$

where  $f_j$  denotes the cut-off frequency of  $j$ -th element of switching function (or control input).

The equivalent control input that holds the states onto the settling sliding surface can be obtained by letting

$$\begin{aligned} S(k, i+1) &= \alpha S(k, i) \\ &\Leftrightarrow Gx(k, i+1) + Gx_r(k, i+1) \\ &= \alpha Gx(k, i) + \alpha Gx_r(k, i) \\ &\Leftrightarrow G\{\Phi_m x(k, i) + \Gamma_m u(k, i)\} + Gx_r(k, i+1) \\ &= \alpha Gx(k, i) + \alpha Gx_r(k, i). \end{aligned} \quad (26)$$

From the above equation, we obtain the following equivalent control input.

$$\begin{aligned} u_{\text{eq}}(k, i) &= -(G\Gamma_m)^{-1}(G\Phi_m - \alpha G)\hat{x}(k, i) \\ &\quad - (G\Gamma_m)^{-1}\{Gx_r(k, i+1) - \alpha Gx_r(k, i)\}, \end{aligned} \quad (27)$$

where the current state estimator is used in the above equation.

The hyperplane matrix  $G$  can be thought of as a state feedback gain, and it can be determined in the  $H_2$  sense in order to minimize the error from the ideal sliding hyperplane by solving the following discrete algebraic Riccati equation (Utkin and Young 1977).

$$\begin{aligned} \Phi_\varepsilon^T P \Phi_\varepsilon - P - \Phi_\varepsilon^T P \Gamma_m (\Gamma_m^T P \Gamma_m)^{-1} \Gamma_m^T P \Phi_\varepsilon + W &= 0 \\ G &= \Gamma_m^T P, \end{aligned} \quad (28)$$

where  $P$  is the unique solution of Eq. 28,  $W$  is a weighting, and  $\Phi_\varepsilon$  is a modified system matrix (Chen et al. 1989) with stability margin  $\varepsilon$  defined as follows:

$$\Phi_\varepsilon := \Phi_m + \varepsilon I, \quad 0 \leq \varepsilon < 1. \quad (29)$$

With this modified system matrix associated with  $\varepsilon$ , we can design  $G$  such that the spectral radius of the closed-loop system other than  $\alpha$  be less than  $1 - \varepsilon$ . This implies that the cut-off frequency of associated modes can be described with  $\varepsilon$  as follows:

$$f_{\text{co}} \geq -\frac{\log_e(1 - \varepsilon)}{2\pi T_m} \quad (30)$$

### 2.4 Combined linear equivalent system

Regarding the combined linear equivalent dynamics of multi-rate system, substituting  $u$  in Eq. 2 by the expression in Eq. 27 as well as letting  $w$  of Eq. 2 and  $x_r$  of Eq. 27 be zero, we have the following equation.

$$x(k, i+1) = \Phi_m x(k, i) + \Gamma_m K_{\text{eq}} \hat{x}(k, i) \quad (31)$$

$$K_{\text{eq}} := -(G\Gamma_m)^{-1}(G\Phi_m - \alpha G), \quad K_{\text{eq}} \in \mathbf{R}^{m \times n}. \quad (32)$$

From Eqs. 31 and 32, we have

$$x(k+1, 0) = \Phi_{\text{eq}}^r x(k, 0) - \sum_{j=0}^{r-1} \Phi_{\text{eq}}^{r-1-j} \Gamma_m K_{\text{eq}} \hat{e}(k, j), \quad (33)$$

$$\Phi_{\text{eq}} := (\Phi_m + \Gamma_m K_{\text{eq}}), \quad \Phi_{\text{eq}} \in \mathbf{R}^{n \times n}. \quad (34)$$

By substituting the Eq. 33 for Eq. 15, we have

$$\begin{aligned} x(k+1, 0) &= \Phi_{\text{eq}}^r x(k, 0) \\ &\quad - \sum_{j=0}^{r-1} \Phi_{\text{eq}}^{r-1-j} \Gamma_m K_{\text{eq}} \Phi_{\text{obs11}}(j) \hat{e}(k, 0) \\ &\quad - \sum_{j=0}^{r-1} \Phi_{\text{eq}}^{r-1-j} \Gamma_m K_{\text{eq}} \Phi_{\text{obs12}}(j) z(k-1, 0). \end{aligned} \quad (35)$$

Therefore, the overall combined dynamics of Eqs. 15 and 35 can be written as follows:

$$\begin{bmatrix} \hat{e}_z(k+1) \\ x(k+1,0) \end{bmatrix} = \begin{bmatrix} \Phi_{obs} & O \\ E & \Phi_{eq}^r \end{bmatrix} \begin{bmatrix} \hat{e}_z(k) \\ x(k,0) \end{bmatrix}$$

$$E := -\sum_{j=0}^{r-1} \Phi_{eq}^{r-1-j} \Gamma_m K_{eq} \begin{bmatrix} \Phi_{obs11}^T(j) \\ \Phi_{obs12}^T(j) \end{bmatrix}^T \quad (36)$$

This eigenstructure shows that  $G$  and  $L$  can be designed separately. Note that  $G$  can be designed such that  $G\Gamma$  is nonsingular without any serious difficulty since  $B$  is full rank by assumption. Also, it should be pointed out that  $G$  and  $\alpha$  can be designed separately.

### 3 Experimental results

#### 3.1 Sinusoidal response and reference tracking

First, we have carried out some experiments to check if our method works properly, using a 3.5 in. 15 kHz-sampling 7,200 rpm low profile HDD, driven by a floating point DSP (TMS320C6711) equipped with 14 bit ADC, 12 bit DAC. The design specifications are shown in Table 1. In this pre-check experiment, we considered only the VCM gain perturbation of 30 and compared an sinusoidal response. Experiment for pivot nonlinearity compensation will follow (Fig. 3).

The equivalent multi-rate plant model for design can be described as follows.

$$\Phi_m = \begin{bmatrix} 1 & T_m \\ 0 & 1 \end{bmatrix}, \quad \Gamma_m = K_f \begin{bmatrix} T_m^2/2 \\ T_m \end{bmatrix}, \quad C = [1 \ 0]. \quad (37)$$

For the estimator, the selection of proportional and integral gain are made so that they have characteristics of 3 kHz Butterworth and 100 Hz respectively. The corresponding pole locations are  $[0.2593 + 0.3192i, 0.2593 - 0.3192i, 0.9590]$ . Utilizing Ackerman's formula (Franklin et al. 1998) for direct pole placement, from Eq. 17 we have the following estimation gain.

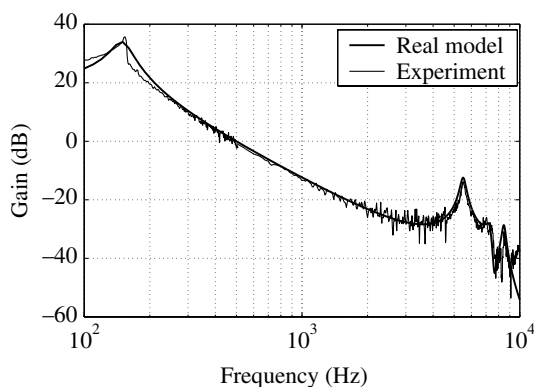


Fig. 3 Frequency response of actuator(VCM)

Table 1 Drive specifications

Sampling freq.	$1/T_s$	15 kHz
Control updating freq. <td><math>1/T_m</math></td> <td>45 kHz</td>	$1/T_m$	45 kHz
Multi-rate ratio	$r$	3
VCM gain	$K_f$	$1 \times 10^4$
Time delay	$T_d$	20 us
Track per inch	TPI	76200TPI

$$L_{mr} = \begin{bmatrix} 3.5386 \times 10^{-1} & 3.3564 \times 10^3 \end{bmatrix}^T, \quad (38)$$

$$K = 6.0045 \times 10^2.$$

Regarding the regulator,  $f$  in Eq. 25,  $f_{co}$  in Eq. 30, and  $W$  in Eq. 28 are selected as 1 kHz, 1 kHz, and  $diag(1,1)$ , respectively, and we have a following sliding hyperplane.

$$G = [2.7920 \times 10^4 \quad 3.4652.] \quad (39)$$

Regarding the uncertainty, including nonlinearity, we consider the simple gain perturbation. The perturbation can be thought of as a parameter uncertainty in the input distribution matrix  $\Gamma_m$ , and thus  $w$  can be modelled as follows:

$$w(k,i) = \Gamma_m (K_r - K_f) u(k,i), \quad (40)$$

where  $K_r$  is a real gain and  $K$  is a nominal gain. From the above  $w$ , we can easily design the discontinuous component of Eq. 8 as follows:

$$v'(k,0) = -\{|K_g - K_f|_{max}|u|\} \frac{C_z \bar{e}_z(k,0)}{|C_z \bar{e}_z(k,0)| + \delta}, \quad (41)$$

where, in the experiments,  $v'$  is filtered by a low pass filter (cutoff frequency is 2 kHz) to generate  $v$  in Eq. 8, and  $\delta$  is a design parameter for a saturation function that alleviates chattering.

To check the closed-loop frequency response for the linear part, the eigenvalues are calculated from Eq. 36, and we have  $[0.959, 0.658, 0.584, 0.259 + 0.319i, 0.259 - 0.319i]$ , which show our desired characteristics.

In Fig. 4, simulations as well as experimental results of open-loop frequency responses are depicted.

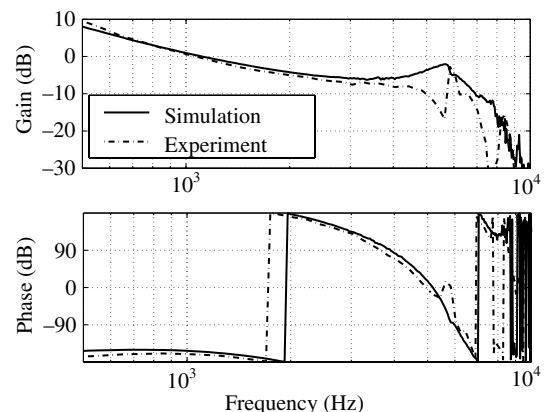


Fig. 4 Open-loop frequency response

Regarding the simulation result, since it is not easy to get a linearized model for variable structure driven system, we used a transfer function estimation technique (Welch, 1967). Although there is a little difference between simulation and experimental results caused by the difference of characteristics of resonant modes, there is no noticeable chattering effect due to the variable structure controller. The open-loop zero crossing frequency was around 1 kHz.

In Fig. 5, we compared the typical sinusoidal response to a 500Hz reference signal for a conventional multi-rate controller (Hara and Tomizuka, 1998) against that for our proposed controller. Notice that letting  $K=0$  and  $\kappa=0$  in our proposed controller yields the conventional one. As it can be seen from this figure, with the conventional controller, the estimation error cannot be ignored when the VCM gain is perturbed. Our proposed controller achieved almost the same performance as the nominal case. Estimation error is suppressed to the same level as the nominal case as shown in Fig. 6. Moreover, in order to check if there is detrimental effect in higher frequency range, we carried out a similar experiment for 5 kHz reference signal. Figure 7 compares the results. As we can see from this figure, no big difference can be observed between proposed and conventional estimator, which implies that the introduced band-limit filter to the discontinuous action actually rejects the higher frequency disturbance and we can alleviate the chattering motion problem.

We then conducted eight tracks seeking experiments and compared the results. Figure 8 shows the forward and backward seeking responses (five times each) for conventional and proposed controllers with  $-30\%$  perturbation of VCM actuator gain. Our proposed method achieves a 1ms seek time, while conventional controller takes almost 2.5 ms because of the presence of residual vibrations. In this experiment, we used a reference trajectory designed such that the jerk during the seek is

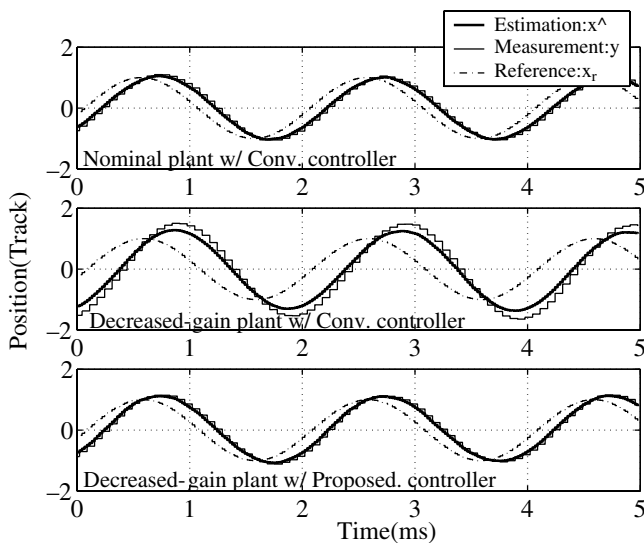


Fig. 5 Comparison of position signal

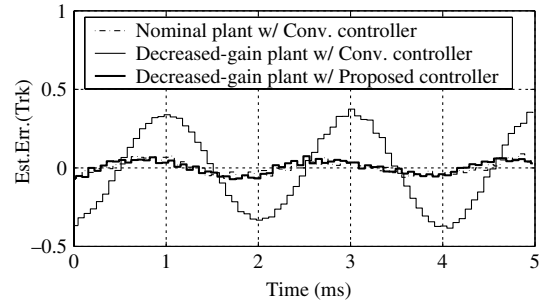


Fig. 6 Comparison of estimation error

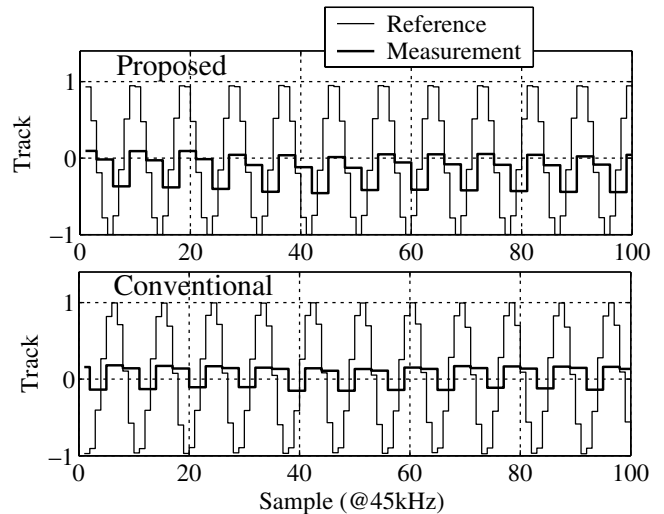


Fig. 7 Comparison of position signal for 5 kHz response

minimized (Mizoshita et al. 1996). No other feedforward compensation was applied. Figure 9 compares the corresponding estimation error. As can be seen from this figure, the estimation error of the proposed control system is much smaller than that of conventional control system, and this results in a decrease of residual vibration.

### 3.2 Practical seeking with pivot nonlinearity compensation

The nonlinearity discussed in the previous subsection was what we intentionally introduced to check the performance. However, it is not that easy to identify or find a best approximation of upper bound for a real nonlinearity which is subject to uncertainty. Moreover, the upper bound of the resulting estimation error space cannot be arbitrarily designed small enough as Eq. 22 implies. Therefore, a trial and error method is required to find the best compensation performance.

First, we began by investigating the “symptoms”. Figure 10 shows both successful and a failure examples of a full stroke seeking operation performed on a drive.

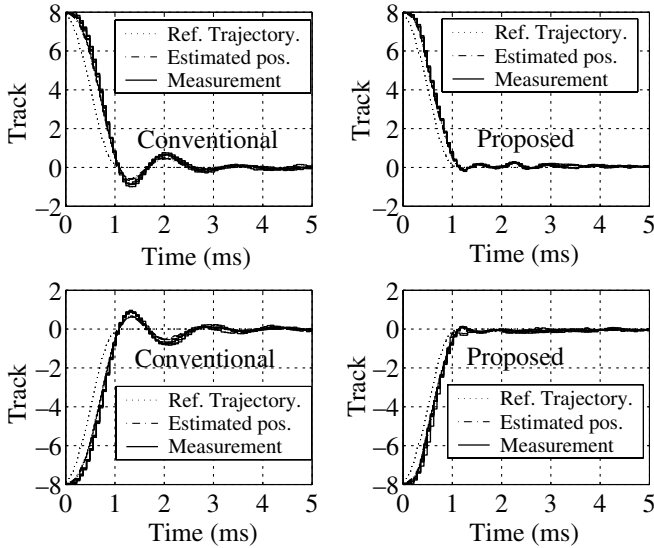


Fig. 8 Comparison of 8-track seek responses for perturbed plant

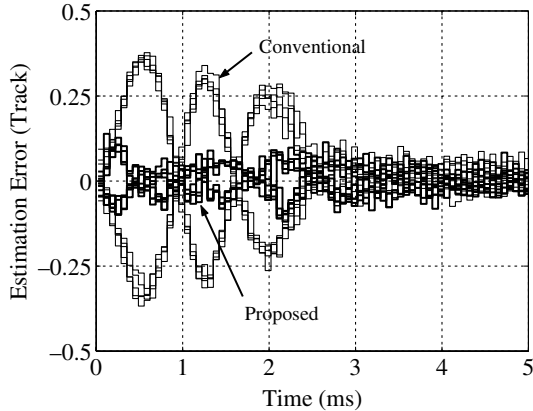


Fig. 9 Estimation error in Fig. 8

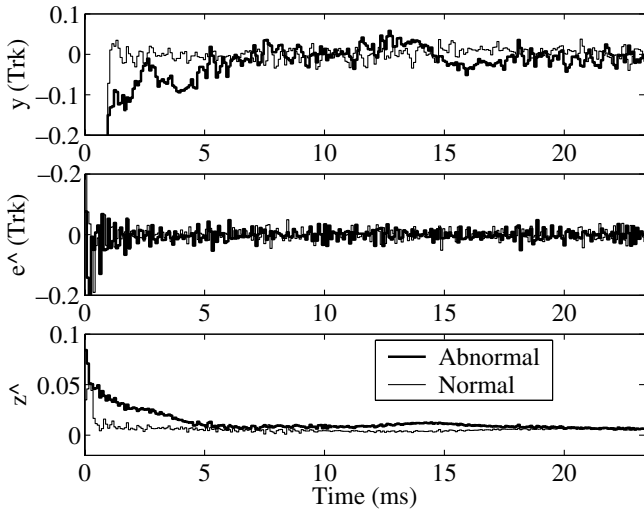


Fig. 10 Comparison of measurement  $y$ , estimation error  $e$ , and integral state  $z$  for different ambient temperature

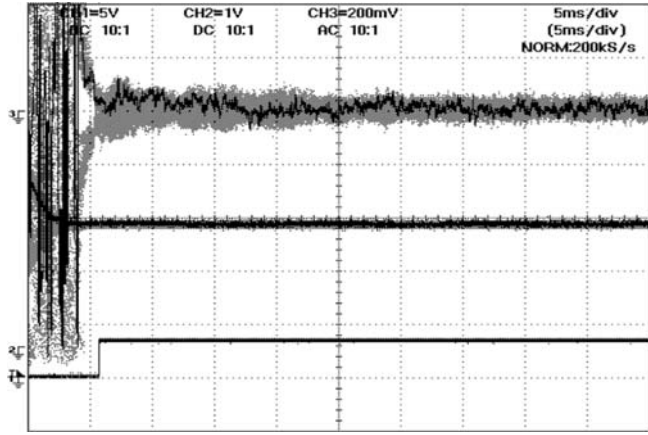


Fig. 11 Random distance seeking operation without VSME

Bold solid lines of all three figures are the results of the seek failure case, operated under a special temperature condition, which is suspected to trigger increased pivot nonlinearity. Thin solid lines represent the seek success case when the drive is operated under normal conditions. Horizontal axes in all three figures are time from the beginning of the settling control. The top figure depicts the head position, from which we can see that the head is not settled for more than 5 ms under the severe condition. The middle figure shows the current estimation error, which does not give any significant difference. The bottom figure is the result of integral state  $\hat{z}$ .

From these time-domain responses, we can see that the most sensitive variable is a integral state  $\hat{z}$ . So the following discontinuous function was selected to compensate for this nonlinearity.

$$v'(k, 0) = -\gamma|\hat{z}(k, 0)| \frac{C_z \bar{e}_z(k, 0)}{|C_z \bar{e}_z(k, 0)| + \delta} \tag{42}$$

where  $\gamma$  is a design parameter. As was used in the previous subsection, we utilized a low pass filter of 2 kHz cutoff frequency to safely feed this back to the estimator.

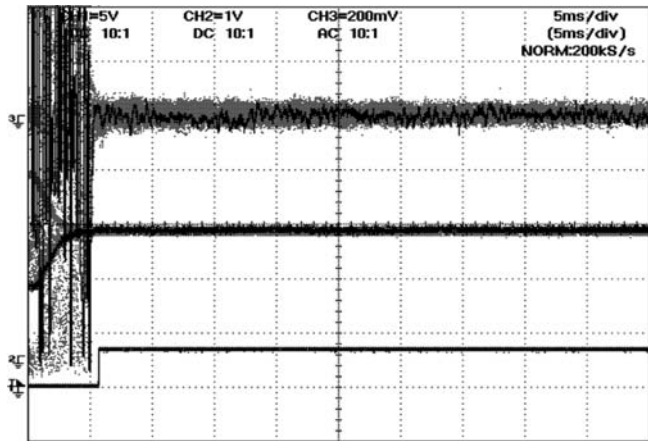


Fig. 12 Random distance seeking operation with VSME

Using this function, random distance seeking operations were carried out for more than 1,000 strokes under a special ambient temperature condition. Figures 11 and 12 respectively depict the resulting responses for the cases without and with the VSME. The upper line on each figure is a fine-scaled head position ( $\pm 1$  track), the middle line is a coarse-scaled head position, and the bottom line is a software flag that is set high when the seeking operation is completed. It is clear from these figures that the settling time is reduced with the use of the VSME and no noticeable problems be observed from these results.

The off-track probability after seeking, which is defined by the number of failures over all trials, is much reduced to less than 1%, while that of a conventional linear controller is 12%. Seek failure occurs when the position cannot be maintained within  $\pm 2.5\%$  of a track pitch for a certain duration after track seeking mode.

---

#### 4 Conclusion

In this paper, we have discussed a way to design a robust seeking control of HDDs by the use of the VSME. The VSME estimates a class of uncertain disturbances and nonlinearities and yields compensation current through the linear feedback gain, which reduces the residual vibration and error during settling. Several experiments were carried out on several drives including a 3.5 in. 7,200 rpm drive. These experiments confirmed that the off-track probability after settling, which is defined by the number of seek failures over all trials, is much reduced to less than 1% even under a special operating temperature condition which increases pivot nonlinearity, while that of a conventional linear controller is 12%. The seek failure is defined as the case when the position cannot be maintained within  $\pm 2.5\%$  of a track pitch for a certain duration after track seeking mode.

---

#### References

- Beale S, Shafai B (1989) Robust control design with a proportional integral observer. *Int J Control* 50:
- Chen YF, Ikeda H, Mita T, Wakui S (1989) Trajectory control of robot arm using sliding mode control and experimented results. *J Robotics Soc Jpn* 7(6):62–67
- Chiang WW (1990) Multirate state-space digital controller for sector servo systems. In: *Proceedings of the 29th IEEE conference on decision and control*, pp 1902–1907
- Franklin GF, Powell JD, Workman M (1998) *Digital control of dynamic systems*, 3rd edn. Addison Wesley, pp 286–287
- Hara T, Tomizuka M (1998) Multi-rate controller for hard disc drive with redesign of state estimator. In: *Proceedings of the American control conference*, pp 898–903
- Ishikawa J (2000) A Study on multirate sampled-data control for hard disk drives. In: *The papers of technical meeting on industrial instrumentation and control*, IEE Japan, IIC-00-55, pp 31–38
- Ishikawa J, Tomizuka M (1998) Pivot friction compensation using an accelerometer and a disturbance observer for hard disk drives. *Transact Mechatron* 3(3): 194–201
- Mizoshita Y, Hasegawa S, Takaishi K (1996) Vibration minimized access control for hard disk drives. *IEEE Trans Mag* 32(3): 1793–1798
- Nakagawa S, Hamada Y (1996) Compensation of frictional force at the head actuator bearing of HDD by using friction observer (Japanese). In: *Proceedings of the Japan Society of Mechanical Engineers WAM*, vol. IV, pp. 594–595
- Ohno K, Abe Y, Maruyama T (2001) Robust following control design for hard disk drives. In: *Proceedings of the IEEE conference on control applications*, pp 930–935
- Prater WL, Stone GJ, Tierney R (1996) Servo Performance of actuator bearing grease. In: *Proceedings of the ASME WAM ISPS-vol 2*, pp 131–137.
- Semba T (2001) An  $H_\infty$  design method for a multi-rate servo controller and applications to a high density hard disk drive. In: *Proceedings of the 40th IEEE conference on decision and control*, pp 4693–4698
- Shafai B, Carroll RL (1985) Design of proportional integral observer for linear time-varying multivariable systems. In: *Proceedings of IEEE conference on decision and control*, pp 597–599
- Takiguchi M, Hirata M, Nonami K (2002) Following control of hard disk drives using multi-rate  $H_\infty$  control. In: *Proceedings of SICE annual conference*
- Utkin VI, Young KD (1977) Methods for constructing discontinuous planes in multidimensional variable structure systems. *Automat Remote Cont* 31:1466–1470
- Walcott BL, Zak SH (1987) State observation of nonlinear uncertain dynamical systems. *IEEE Trans Automatic Cont* 32:166–170
- Welch PD (1967) The use of fast Fourier transform for the estimation of power spectra: a method based on time averaging over short, modified periodograms. *IEEE Trans Audio Electroacoust* AU-15:70–73